

## Magnetic, dielectric, and transport properties of $\text{La}_{1-x}\text{Sr}_x\text{MnO}_3$ at submillimeter wavelengths

V. Yu. Ivanov, V. D. Travkin, A. A. Mukhin, S. P. Lebedev, A. A. Volkov, Andrei Pimenov, Alois Loidl, A. M. Balbashov, A. V. Mozhaev

### Angaben zur Veröffentlichung / Publication details:

Ivanov, V. Yu., V. D. Travkin, A. A. Mukhin, S. P. Lebedev, A. A. Volkov, Andrei Pimenov, Alois Loidl, A. M. Balbashov, and A. V. Mozhaev. 1998. "Magnetic, dielectric, and transport properties of  $\text{La}_{1-x}\text{Sr}_x\text{MnO}_3$  at submillimeter wavelengths." *Journal of Applied Physics* 83 (11): 7180–82. <https://doi.org/10.1063/1.367675>.



RESEARCH ARTICLE | JUNE 01 1998

## Magnetic, dielectric, and transport properties of $\text{La}_{1-x}\text{Sr}_x\text{MnO}_3$ at submillimeter wavelengths

V. Yu. Ivanov; V. D. Travkin; A. A. Mukhin; S. P. Lebedev; A. A. Volkov; A. Pimenov; A. Loidl; A. M. Balbashov; A. V. Mozhaev



*J. Appl. Phys.* 83, 7180–7182 (1998)


<https://doi.org/10.1063/1.367675>




View  
Online




Export  
Citation



Lock-in Amplifier



Boxcar Averager



Zurich  
Instruments

Boost Your Optics and  
Photonics Measurements

Find out more

# Magnetic, dielectric, and transport properties of $\text{La}_{1-x}\text{Sr}_x\text{MnO}_3$ at submillimeter wavelengths

V. Yu. Ivanov, V. D. Travkin, A. A. Mukhin,<sup>a)</sup> S. P. Lebedev, and A. A. Volkov  
General Physics Institute of the Russian Academy of Science, 38 Vavilov Street, 117942 Moscow, Russia

A. Pimenov and A. Loidl  
Experimentalphysik V, Universitat Augsburg, D-86159 Augsburg, Germany

A. M. Balbashov and A. V. Mozhaev  
Moscow Power Engineering Institute, 14 Krasnokazarmennaya Street, 105835 Moscow, Russia

Antiferromagnetic resonance (AFMR), dynamic conductivity, and dielectric permittivity have been studied in the  $\text{La}_{1-x}\text{Sr}_x\text{MnO}_3$  perovskites at a frequency range of  $\nu = 3\text{--}33\text{ cm}^{-1}$  by the use of a quasi-optical backward-wave-oscillator technique. Two AFMR modes have been observed in  $\text{LaMnO}_3$  and  $\text{La}_{0.95}\text{Sr}_{0.05}\text{MnO}_3$ . Temperature dependencies of their resonance frequencies, linewidths, and mode contributions to a static magnetic permeability have been obtained and corresponding parameters of magnetic interactions have been extracted. A jump in the dielectric permittivity  $\epsilon'(T)$  was found at  $T = 100\text{--}120\text{ K}$  in  $\text{La}_{0.9}\text{Sr}_{0.1}\text{MnO}_3$ , which indicates the existence of an additional phase transition (probably, a polaron ordering) besides the ferromagnetic transition at  $170\text{ K}$ . A sharp increase of the dynamic conductivity  $\sigma'(\nu, T)$  was observed near Curie temperature ( $285\text{ K}$ ) at a metal–semiconductor transition in  $\text{La}_{0.825}\text{Sr}_{0.175}\text{MnO}_3$ , which was slightly smaller than its static value. © 1998 American Institute of Physics. [S0021-8979(98)31811-3]

The recent observation of the colossal negative magnetoresistance in doped perovskites  $\text{R}_{1-x}\text{A}_x\text{MnO}_3$ , where R is a trivalent rare-earth ion and A is a divalent ion such as Ca or Sr,<sup>1</sup> has attracted considerable interest in these compounds. Their magnetic, electronic transport, structural, and optical properties exhibit a remarkable variation with the doping level.<sup>2–4</sup>

The parent compound  $\text{LaMnO}_3$  (Mott-type insulator) has a canted antiferromagnetic layer ( $A_yF_z$ ) structure with a Neel temperature  $T_N \approx 140\text{ K}$ .<sup>5–7</sup> Manganese ions  $\text{Mn}^{3+}$  have a  $3d^4$  electronic configuration with a total spin  $S=2$ , where three electrons occupying  $t_{2g}$  orbitals may be considered as a local spin of  $S=3/2$ , while the remaining electron occupies an  $e_g$  orbital hybridized with oxygen  $2p$  states. The spins of the  $t_{2g}$  and  $e_g$  electrons are parallel aligned due to on-site Hund coupling. The substitution of the rare-earth ions by Sr (or Ca) ions results in doping of holes to the  $e_g$  orbitals and a transition from a canted antiferromagnetic insulating state to a ferromagnetic metallic state,<sup>1,2,8</sup> which is stabilized due to a double exchange.<sup>9</sup>

Recent spectroscopic investigations of the doped lanthanum manganites indicate that their dynamic properties change drastically through the phase transitions and are very sensitive to the doping level. An infrared study of the optical conductivity of  $\text{La}_{1-x}\text{Sr}_x\text{MnO}_3$  has shown a large variation of the electronic structure in a wide frequency range ( $\sim 2\text{ eV}$ ) with the spin polarization of the conduction carriers<sup>4</sup> and a shift of phonon frequencies at the ferromagnetic metal–insulator transition.<sup>10</sup> Inelastic neutron scattering experiments have revealed spin excitations in pure  $\text{LaMnO}_3$ ,<sup>7,11</sup> and these dramatically change with doping level.<sup>12</sup> In this work we performed investigations of antifer-

romagnetic resonance (AFMR), dynamic conductivity, and dielectric permittivity of  $\text{La}_{1-x}\text{Sr}_x\text{MnO}_3$  manganites in the submillimeter frequency range by means of a quasi-optical backward-wave-oscillator technique.<sup>13,14</sup>

Single crystals of  $\text{La}_{1-x}\text{Sr}_x\text{MnO}_3$  ( $x = 0, 0.05, 0.1, 0.15$ , and  $0.175$ ) were grown by the floating zone method with radiation heating in an air atmosphere. X-ray powder diffraction measurements showed that grown materials were of single phase. However, x-ray topography has revealed a twin structure in the crystals.

Resistance,  $\rho(T)$ , was measured using the four-probe method at  $T = 4.2\text{--}400\text{ K}$  in magnetic fields  $H$  up to  $12\text{ kOe}$ . Magnetization  $M(T, H)$  and ac magnetic susceptibility  $\chi_{ac}(T)$  measurements were performed in magnetic fields  $H \leq 12\text{ kOe}$  at  $T = 4.2\text{--}400\text{ K}$ .

The transmission  $T(\nu)$  and phase shift  $\Delta\varphi(\nu)$  spectra of thin plane-parallel plates were measured using a quasi-optical submillimeter backward-wave-oscillator spectrometer<sup>13,14</sup> in the frequency range  $\nu = 3\text{--}33\text{ cm}^{-1}$  at temperatures of  $5\text{--}300\text{ K}$ . The complex dielectric permittivity  $\epsilon(\nu, T) = \epsilon' + i\epsilon''$  as well as the dynamic conductivity  $\sigma(\nu, T)$  were determined from the  $T(\nu)$  and  $\Delta\varphi(\nu)$  spectra using Fresnel's formulas for the transmission and phase shift of the plane-parallel plate.<sup>15</sup> In order to take into account the AFMR mode contribution we used a harmonic oscillator model for a permeability dispersion:

$$\mu = 1 + \sum_i \Delta\mu_i \nu_i^2 / (\nu_i^2 - \nu^2 + j\nu\Delta\nu_i), \quad (1)$$

where  $\nu_i$ ,  $\Delta\nu_i$ , and  $\Delta\mu_i$  are the resonance frequency, linewidth, and mode contribution to the static permeability of the  $i$ th mode, respectively,  $j = \sqrt{-1}$ .

**LaMnO<sub>3</sub>:** In the transmission spectra of the pure  $\text{LaMnO}_3$  we observed two lines close together, which appeared at  $T < T_N = 140\text{ K}$ . We have identified the lines with

<sup>a)</sup>Electronic mail: mukhin@ss.gpi.ru

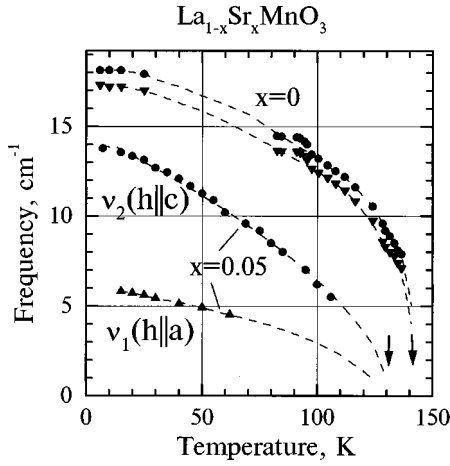


FIG. 1. Temperature dependence of the AFMR frequencies in  $\text{LaMn}_{1-x}\text{Sr}_x\text{O}_3$  for  $x=0$  and  $0.05$ . Arrows indicate the corresponding Neel temperatures.

two AFMR modes and have fitted  $T(\nu)$  spectra using Fresnel's formulas and Eq. (1) for the permeability. The temperature dependence of the AFMR frequencies is shown in Fig. 1. The values of the linewidth, mode contribution, and complex dielectric permittivity are equal to  $\Delta\nu_{1,2} \approx 0.5 \text{ cm}^{-1}$ ,  $\Delta\mu_{1,2} \approx 0.035$ , and  $\epsilon' \approx 20.5$ ,  $\epsilon'' \approx 0.1$ , respectively, at  $T=80 \text{ K}$ . An inelastic neutron scattering study of  $\text{LaMnO}_3$  gives the gap for the spin waves at about  $19.8 \text{ cm}^{-1}$  at  $20 \text{ K}$  (Ref. 7) and  $19.4 \text{ cm}^{-1}$  at  $8 \text{ K}$ ,<sup>11</sup> in agreement with our resonance frequency values of  $18.1$  and  $17.3 \text{ cm}^{-1}$  at  $4.2 \text{ K}$  (Fig. 1).

According to Refs. 6 and 7 the antiferromagnetic spin axis in  $\text{LaMnO}_3$  is along the  $b$  axis of the orthorhombic Pbnm crystal and a small spin canting takes place along the  $c$  axis (magnetic structure of the  $A_yF_z$  type). There are two AFMR modes in the crystal whose frequencies are determined by<sup>14</sup>

$$\nu_1 = \gamma(2H_E H_A^{cb})^{1/2}, \quad \nu_2 = \gamma(2H_E H_A^{ab} + H_D^2)^{1/2}, \quad (2)$$

where  $H_A^{cb} = K_{cb}/M_0$ ,  $H_A^{ab} = K_{ab}/M_0$ , and  $K_{cb,ab}$  are anisotropy constants for the  $cb$  and  $ab$  crystallographic planes, respectively,  $H_E$  and  $H_D$  are isotropic and antisymmetric exchange fields, respectively,  $M_0/2$  is a sublattice magnetization, and  $\gamma$  is a gyromagnetic ratio. The first (quasiferromagnetic) mode is excited by  $h||a$  and  $b$  axes, while the second (quasiantiferromagnetic) mode is excited by  $h||c$  axis. The corresponding mode contributions are:  $\Delta\mu_1^a = 4\pi\rho\chi_\perp$ ,  $\Delta\mu_1^b = 4\pi\rho\chi_{\text{rot}}$  for mode 1 and  $\Delta\mu_2^c = 4\pi\rho\chi_\perp$  for mode 2, where  $\chi_\perp = M_0/2H_E$  and  $\chi_{\text{rot}} = m_0^2/K_{cb}$  are transverse and rotation susceptibilities, respectively,  $m_0 = \chi_\perp H_D$  is the weak ferromagnetic moment and  $\rho \approx 6.5 \text{ g/cm}^3$  is the crystal density. Due to the twin structure of the investigated  $\text{LaMnO}_3$  crystals both modes were observed simultaneously with nearly equal mode contributions at various polarization of radiation. Assuming equal volume for all six kinds of the twins and their even distribution in the sample we obtain  $\Delta\mu_1 = 1/3(\Delta\mu_1^a + \Delta\mu_1^b)$  and  $\Delta\mu_2 = 1/3\Delta\mu_2^c$  and then we may estimate  $\chi_\perp \approx (1.4 \pm 0.2) \times 10^{-4} \text{ cm}^3/\text{g}$  and the corresponding exchange field  $H_E \approx 3.3 \times 10^5 \text{ Oe}$ . This value of the  $\chi_\perp$  is in a reasonable agreement with the  $\chi_\perp = (1.8 \pm 0.3)$

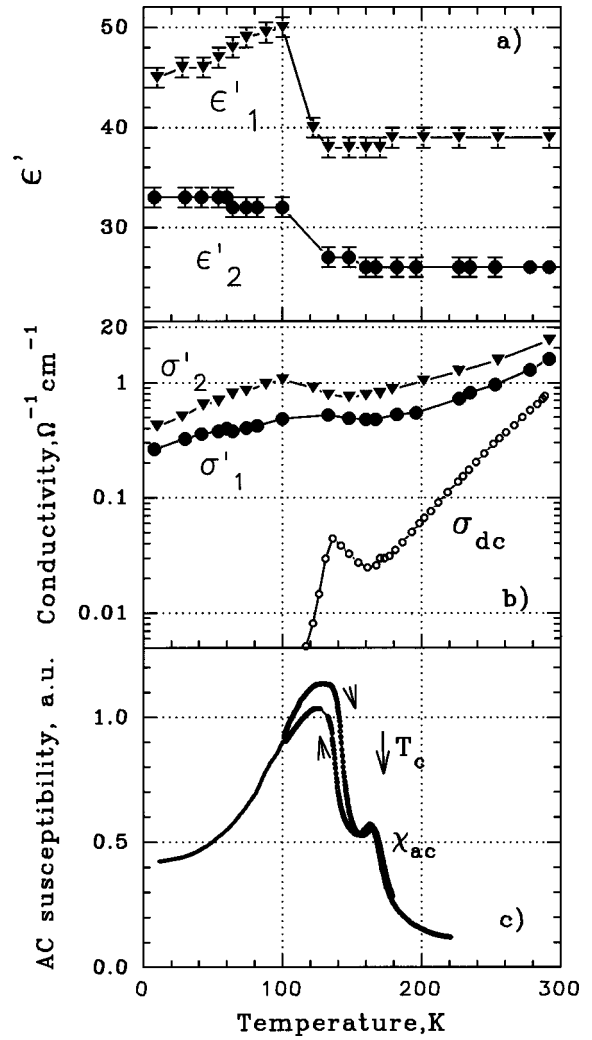


FIG. 2. Temperature dependence of the dielectric permittivity  $\epsilon'_{1,2}(7.5 \text{ cm}^{-1})$  (a), dynamic  $[\sigma'_{1,2}(7.5 \text{ cm}^{-1})]$  and static ( $\sigma_{d0}$ ) conductivity (b) and ac magnetic susceptibility  $\chi_{ac}$  (c) of  $\text{La}_{0.95}\text{Sr}_{0.05}\text{MnO}_3$ . Indices 1,2 correspond to the two crystallographic directions: 1— $[-110]$  and 2— $[11-2]$ .

$\times 10^{-4} \text{ cm}^3/\text{g}$  deduced from our static measurements. Using the interplane exchange constant obtained from an inelastic neutron scattering study of the spin waves in  $\text{LaMnO}_3$ ,<sup>7,11</sup> we can determine  $H_E \approx 4 \times 10^5 \text{ Oe}$  that is close to our data. Using the value of the weak ferromagnetic moment for a single domain  $m_0(T=78 \text{ K}) = 4.2 \pm 0.5 \text{ emu/g}$  deduced from our static measurements and anisotropy constant  $K_{cb}(T=78 \text{ K}) \approx 3 \times 10^6 \text{ erg/g}$  ( $\approx 6 \text{ cm}^{-1}/\text{ion}$ ) determined from the AFMR frequency we may estimate  $\chi_{\text{rot}} = 6 \times 10^{-6} \text{ cm}^3/\text{g}$ . The small value of the  $\chi_{\text{rot}}$ , i.e.,  $\chi_{\text{rot}} \ll \chi_\perp$ , explains the nearly equal mode contributions ( $\Delta\mu_1 \approx \Delta\mu_2$ ) observed in our experiment. We note also the small contribution of the antisymmetric exchange field  $H_D$  into the AFMR frequency and nearly equal values of the anisotropy constants in different crystallographic planes that permit the use of a simple model of an uniaxial antiferromagnet to describe the spin waves in  $\text{LaMnO}_3$ .<sup>7,11</sup>

**$\text{La}_{0.95}\text{Sr}_{0.05}\text{MnO}_3$ :** Two AFMR modes were revealed for this composition, which in contrast to the pure  $\text{LaMnO}_3$ , had significantly different frequencies (Fig. 1). What's more, the

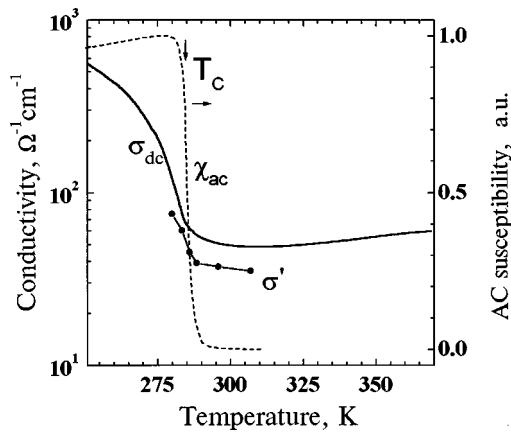


FIG. 3. Temperature dependence of the dynamic  $\sigma'_{1,2}$  (at  $7\text{--}20\text{ cm}^{-1}$ ) and static ( $\sigma_{dc}$ ) conductivity and ac magnetic susceptibility ( $\chi_{ac}$ ) of  $\text{La}_{0.825}\text{Sr}_{0.175}\text{MnO}_3$ .

samples (*b*-cut plane parallel plates) practically did not contain twins and we were able to determine excitation conditions and identify the modes: the low frequency mode ( $\nu_1$ ) observed at the  $h\parallel a$  axis was identified as a quasiferromagnetic mode, while the high frequency mode ( $\nu_2$ ) excited by the  $h\parallel c$  axis was identified as a quasiantiferromagnetic one. The values of the mode contributions and linewidths are ( $T = 10\text{ K}$ ):  $\Delta\mu_1 = 0.016 \pm 0.003$ ,  $\Delta\mu_2 = 0.015 \pm 0.003$ ,  $\Delta\nu_{1,2} \approx 2\text{ cm}^{-1}$ .

We assumed above that the magnetic structure is of the  $A_yF_z$  type. This conclusion is confirmed by the neutron scattering and magnetic study of the  $\text{La}_{0.96}\text{Sr}_{0.04}\text{MnO}_3$ ,<sup>16</sup> where the magnetic structure remains similar to that of pure  $\text{LaMnO}_3$ , however, with increased value of a canting angle. According to our static measurements of  $\text{La}_{0.95}\text{Sr}_{0.05}\text{MnO}_3$  the magnetic susceptibilities  $\chi_a \approx \chi_c = (1.3\text{--}1.9) \times 10^{-4}\text{ cm}^3/\text{g}$ ,  $\chi_b = (5.3 \pm 0.5) \times 10^{-4}$ , and spontaneous moment along the *c* axis  $m_0 = 18 \pm 4\text{ emu/g}$  are in agreement with the  $A_yF_z$  magnetic structure. However, we note a noticeable increase (about four times) of the canting angle and significant decrease of the anisotropy constant in the *cb* plane. The estimated values of the  $K_{cb}$  are:  $(0.7 \pm 0.2) \times 10^6\text{ cm}^3/\text{g}$  from the AFMR data and  $(0.6 \pm 0.2) \times 10^6\text{ cm}^3/\text{g}$  from the rotation susceptibility ( $\chi_b$ ).

The dielectric properties of  $\text{La}_{0.95}\text{Sr}_{0.05}\text{MnO}_3$  are similar to  $\text{LaMnO}_3$ , however we note their anisotropy and higher dielectric losses, in particular,  $\epsilon'_a \approx 24$ ,  $\epsilon''_a = 0.6\text{--}0.7$ , and  $\epsilon'_c \approx 20$ ,  $\epsilon''_c \approx 0.2\text{--}0.3$  for  $\nu = 5\text{--}13\text{ cm}^{-1}$  and  $T = 80\text{ K}$ .

**$\text{La}_{0.9}\text{Sr}_{0.1}\text{MnO}_3$ :** Magnetic, dielectric, and transport properties of this composition suffer significant changes as compared with previous ones. We did not observe magnetic modes in the range  $5\text{--}20\text{ cm}^{-1}$  since the magnetic ordering at  $T < T_C \approx 170\text{ K}$  is of the ferromagnetic type and a ferromagnetic resonance is expected at much lower frequencies. However, apparent anomalies were observed in the temperature dependence of the dielectric permittivity and conductivity (Fig. 2). A pronounced jumplike behavior for  $\epsilon'(T)$  and a maximum for  $\sigma'(T)$  between 100 and 120 K indicate the existence of an additional phase transition besides the magnetic transition at  $T_C$ . The anomalous behavior of the ac magnetic susceptibility at  $T < T_C$  [Fig. 2(c)] confirms this

conclusion. One possible origin of this transition may be related to a polaron ordering connected with a freezing of holes on the lattice sites.<sup>17</sup>

We note also an anisotropy of the  $\epsilon'$  and  $\sigma'$  for different crystallographic directions [Figs. 2(a) and 2(b)]. The dynamic conductivity  $\sigma'(T)$  is considerably greater than the static one,  $\sigma_{dc}(T)$  [Fig. 2(b)]. This indicates that not only free charge carriers contribute to the dynamic  $\sigma'$  but also contributions from the localized carriers and crystal lattice are of importance at the submillimeter wavelengths.

**$\text{La}_{0.825}\text{Sr}_{0.175}\text{MnO}_3$ :** For the high conducting composition ( $x = 0.175$ ) a considerable decrease of the transmission  $T(\nu)$  for the  $0.026\text{ mm}$  plate on lowering the temperature was observed near the ferromagnetic phase transition at  $T_C \approx 285\text{ K}$ , accompanied by a metal–semiconductor transition. In particular,  $T$  decreases from  $2 \times 10^{-3}$  at  $300\text{ K}$  to  $10^{-4}$  at  $280\text{ K}$ . The extracted dynamic conductivity  $\sigma'(\nu, T)$  is slightly smaller than its static value  $\sigma_{dc}(T)$  and exhibits a sharp increase at the phase transition (Fig. 3). The main contribution to  $\sigma'(\nu, T)$  is Drude-like, practically without frequency dispersion. The real part of the dielectric permittivity amounts to  $\epsilon'(T = 295\text{ K}) = 37$  and shows no frequency dispersion.

In conclusion, this study of the submillimeter properties of the  $\text{La}_{1-x}\text{Sr}_x\text{MnO}_3$  perovskites shows the intimate relations between their magnetic excitations, charge carriers, and crystal lattice dynamics and gives insight into the origin of their unusual magnetic, electronic, and structural properties.

This work was supported in part by the Russian Foundation for Basic Research (Grant Nos. 97-02-17325 and 96-02-18091) and the Ministry of Science and Technical Policy of the Russian Federation.

- <sup>1</sup>R. von Helmholt, J. Wecker, B. Holzapfel, L. Schultz, and K. Samwer, Phys. Rev. Lett. **71**, 2331 (1993).
- <sup>2</sup>A. Urushibura, Y. Moritomo, T. Arima, A. Asamitsu, G. Kido, and Y. Tokura, Phys. Rev. B **51**, 14103 (1995).
- <sup>3</sup>Y. Okimoto, T. Katsufuji, T. Ishikawa, A. Urushibura, T. Arima, and Y. Tokura, Phys. Rev. Lett. **75**, 109 (1995).
- <sup>4</sup>Y. Okimoto, T. Katsufuji, T. Ishikawa, T. Arima, and Y. Tokura, Phys. Rev. B **55**, 4206 (1997).
- <sup>5</sup>E. O. Wollan and W. C. Koehler, Phys. Rev. **100**, 545 (1955).
- <sup>6</sup>G. Matsumoto, J. Phys. Soc. Jpn. **29**, 606 (1970).
- <sup>7</sup>F. Moussa, M. Hennion, J. Rodriguez-Carvajal, H. Moudden, L. Pinsard, and A. Revcolevschi, Phys. Rev. B **54**, 15149 (1996).
- <sup>8</sup>G. H. Jonker and J. H. van Santen, Physica (Utrecht) **16**, 337 (1950).
- <sup>9</sup>C. Zener, Phys. Rev. **81**, 440 (1951); **82**, 403 (1951).
- <sup>10</sup>K. H. Kim, J. Y. Gu, H. S. Choi, G. W. Park, and T. W. Noh, Phys. Rev. Lett. **77**, 1877 (1996).
- <sup>11</sup>K. Hirota, N. Kaneko, A. Nishizawa, and Y. Endoh, J. Phys. Soc. Jpn. **65**, 3736 (1996).
- <sup>12</sup>M. Hennion, F. Moussa, J. Rodriguez-Carvajal, H. Moudden, L. Pinsard, and A. Revcolevschi, Physica B **234–236**, 851 (1997).
- <sup>13</sup>A. A. Volkov, Yu. G. Goncharov, G. V. Kozlov, S. P. Lebedev, and A. M. Prokhorov, Infrared Phys. **25**, 369 (1985).
- <sup>14</sup>A. M. Balbashov, G. V. Kozlov, A. A. Mukhin, and A. S. Prokhorov, in *High Frequency Processes in Magnetic Materials*, edited by G. Srinivasan and A. Slavin (World Scientific, Singapore, 1995), Chap. 2, pp. 56–98.
- <sup>15</sup>M. Born and E. Wolf, *Principles of Optics*, 4th ed. (Pergamon, Oxford, 1980).
- <sup>16</sup>H. Kawano, R. Kajimoto, M. Kubota, and H. Yoshizawa, Phys. Rev. B **53**, 2202 (1996).
- <sup>17</sup>Y. Yamada, O. Hino, S. Nohdo, R. Kanao, T. Inami, and S. Katano, Phys. Rev. Lett. **77**, 904 (1996).